Contents available at ISC and SID
Journal homepage: www.rangeland.ir

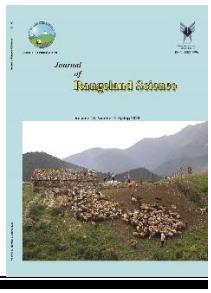

**Research and Full Length Article:**

# Assessing Sensitivity to Desertification Using the Fuzzy Overlay Method in Mashhad, Iran

**Mostafa Dastorani**
Assistant Prof., Faculty of Geography and Environmental Sciences, Hakim Sabzevari University, Sabzevar, Iran, Email: m.dastorani@hsu.ac.ir

Received on: 11/10/2021
Accepted on: 26/02/2022
DOI: 10.30495/RS.2023.689427

**Abstract.** In this research, we used six MODIS remote sensing products to evaluate the vulnerability to desertification in Mashhad, Iran in 2020. The Enhanced Vegetation Index (EVI), Vegetation Condition Index (VCI), Salinity Index (SI), Synthetized Drought Index (SDI), Temperature Condition Index (TCI), and precipitation were considered in May, 2020 when vegetation growth reaches its maximum size. Data layers were standardized using the Fuzzy Transform Function and scaled using the Analytical Hierarchy Process (AHP). Regarding TCI, VCI, and SDI, the greatest proportion of the area fell under the no drought to mild drought category indicating a lower risk of desertification. However, the Synthetized Desertification Index (SDI) was mainly distributed around the moderate and mild classes (~39%). The results of the EVI index also indicated that most of the area had a suitable vegetation density and low risk of desertification. As for the SI index, ~98% happened under the low salinity risk. Based on the results of the Analytical Hierarchy Process (AHP) method, precipitation (0.25), VCI (0.25), EVI (0.18), and SDI (0.13) obtained the greatest weights. The final vulnerability score ranged between 0.29 and 0.63. The results showed that the greatest parts of the area belong to the moderate risk (~68%) and high risk (30.1) classes of desertification. The highest values were obtained in the eastern and southeastern parts of the area with the lowest level of vegetation density, and high-temperature indices. Naturally, the elevations received the lowest values (~0.29) showing an increasing gradient towards the middle plain. The comparison between the results and the ground truth data indicated high compatibility (kappa value of >0.70). Mashhad City as the major population centre of the area is located in the low-risk category; therefore, desertification doesn't seem to be threatening the city at the moment.

**Key words:** Degradation, Land-Use, Vegetation, Salinity, Khorasan

## Introduction

Desertification is not the natural expansion of existing deserts in the definition but the degradation of land in arid, semi-arid, and dry-subhumid areas as the result of human interventions such as overcultivation, overgrazing, deforestation, and poor agricultural activities (Vogt *et al.*, 2011). Desertification has devastating economic, social and environmental impacts not only on-site but even on greater distances (Sivakumar, 2007). This phenomenon was found to be of the utmost priority in the Rio Conference in 1992 which led to the call upon all united nations to establish the specialized convention titled Convention to Combat Desertification to not only understand and evaluate this phenomenon but to find ways to combat or mitigate its consequences (Kjellen, 2003). By the time, drought, salinization and alkalinization of lands due to improper irrigation practices in African Savannah were believed to be the main driving forces of desertification, but later studies proved it wrong (Ma and Zhao, 1994). Nowadays, it is well-established that desertification is a multi-faceted phenomenon affected by or affecting a web of interacting factors (Mouat and Hutchinson, 2012; Egidi and Salvati, 2020; Elhadi and Dano, 2020) and combating it; therefore,it requires a holistic approach in place.

The first step in combating the desertification is understanding the phenomenon *per se* and its consequences. In line with this goal, there have been multiple global and international initiatives for desertification evaluation and mapping such as the Global Assessment of Human-induced Soil Degradation (GLASOD) project at a global scale (Oldeman *et al.*, 1991), and the Mediterranean desertification and land use (MEDALUS) approach (Kosmas *et al.*, 1999) among others. Locally, there have been other attempts to evaluate and zone desertification such as the Iranian Model of Desertification Potential Assessment (IMDPA), Iranian Classification of Desertification (ICD and its modified version MICD) and Iranian Research Institute of Forest and Rangelands Ekhtessasi–Ahmadi (RIFR-EA) model (Fathi *et al.*, 2015). The data-intensity and uncertainties surrounding these models have resulted in a surge of interest in more simplistic but robust approaches such as the integration of satellite imageries and computer based software packages including but not limited to geographic information systems (GIS) into desertification assessments (Albalawi and Kumar, 2013; Gad and Lotfy, 2008). There are numerous cases of applying remote sensing products and GIS tools in desertification assessment such as Jafari *et al.* (2018), Kumar *et al.* (2019), Akbari *et al.* (2020), and Fathizad *et al.* (2018) among others. Moreover, the introduction of statistical and mathematical approaches such as multi-criteria decision making methods (MCDM) into the equation has made these techniques an unprecedented tool for evaluating different environmental issues (Akbari *et al.*, 2021) such as desertification. There has been a growing number of desertification studies by including remote sensing, GIS and MCDM techniques such as Alamdarloo *et al.* (2018), Shihab and Al-hameedawi (2020), Kacem *et al.* (2021), Akbari *et al.* (2021), and Akbari *et al.* (2020). Among the growing body of literature, Aixia *et al.* (2007) evaluated and monitored desertification in China using MODIS and NOAA data by utilizing Modified Soil Adjusted Vegetation Index (MSAVI), Fractional Vegetation Cover (FVC), albedo, Land Surface Temperature (LST) and Temperature Vegetation Dryness Index (TVDI) indices. The authors reported that the indices are useful for large-scale desertification assessment. Lin *et al.* (2009) evaluated desertification intensity in Northwestern China and Mongolia using the MODIS images and Normalized Difference Vegetation Index (NDVI) satellite images. Bezerra *et al.* (2020) used the MODIS Enhanced

Vegetation Index (EVI) for evaluating desertification in Brazilian semiarid areas and found that areas undergoing degradation/desertification increased considerably. In the work of Liu *et al.* (2021), drought impact and desertification were evaluated in Hulun grasslands of China using remote sensing indices including but not limited to NDVI, EVI, Land Surface Temperature (LST), and MSAVI. Despite the existence of multiple studies, yet remote sensing datasets and GIS tools are not well-evaluated for their possible application in assessing desertification. This is attested by the growing number of papers in this regard during the past decade. The gap is more obvious in arid areas suffering from the lack of data and where most of remote sensing data products are not yet enough studied (Sörensson and Ruscica, 2018; Murray *et al.*, 2018). This was the main idea behind conducting this research in an already desertification-stricken area in Iran.

The study area selected for conducting this research is located in an arid part of Iran, with a history of desertification over the past decades. The application of state-of-the-art techniques such as remote sensing and GIS for desertification assessment hasn't been evaluated in this area and we believe this research is the first attempt to bring them all into a comprehensive tool for desertification assessment. The main objective of this research was the application of remote sensing indices in assessing desertification in and arid area of Iran, as well as evaluating the potential of remote sensing indices in detecting land sensitivity to degradation. This study is important given its broad spectrum of remote sensing indices as well as the fact that no similar studies have been conducted in the Mashhad. The results of this research will help land managers to produce desertification maps from free-readily-available sources at no cost. Instead of tedious and cumbersome field works, remote sensing datasets provide an unparalleled tool for land management and land degradation evaluation.

## Materials and Methods

### Study Area

The study area of this research is Mashhad, Khorasan Razavi province, Iran located between 35º 43′ 9″ to 36º 58′ 4″ N and 59º 3′ 48″ and 60º 36′ 21″ E, with a total area of 10326 $km^2$ (Fig. 1). Elevation ranges between 950 m and 1150 m above sea level. The region is characterized by a semi-arid climate going under an annual precipitation of 238 mm with the annual average temperature of 15.7 ºC. The temperature reaches to its maximum of 43ºC in July and its minimum is -23ºC in January. As illustrated in Fig. 2, most of the precipitation is concentrated in the winter and early spring, indicating a Mediterranean climate. Mashhad has a complex geological setting with a number of active faults within its boundaries. Mashhad is bounded to the north by the Kalat and Dargaz, to the east by the Sarakhs plains, to the south by the Torbat Heidarieh and to the west by Neishabour. Based on the results of the census conducted in 2010, Mashhad is home to 3.07 m people mostly concentrated in cities. Mashhad plain is in fact a surrounded valley 100 km in length and 25 km in width as part of the Kashafroud watershed. Geologically, the region is mostly covered with the Karstic and evaporative Mozdouran Sedimentary Carbonates with suitable underground reservoirs. The water table has been dropping over the past decade and most of the rivers and streams have dried out. Location of the study area is illustrated in Fig. 1.

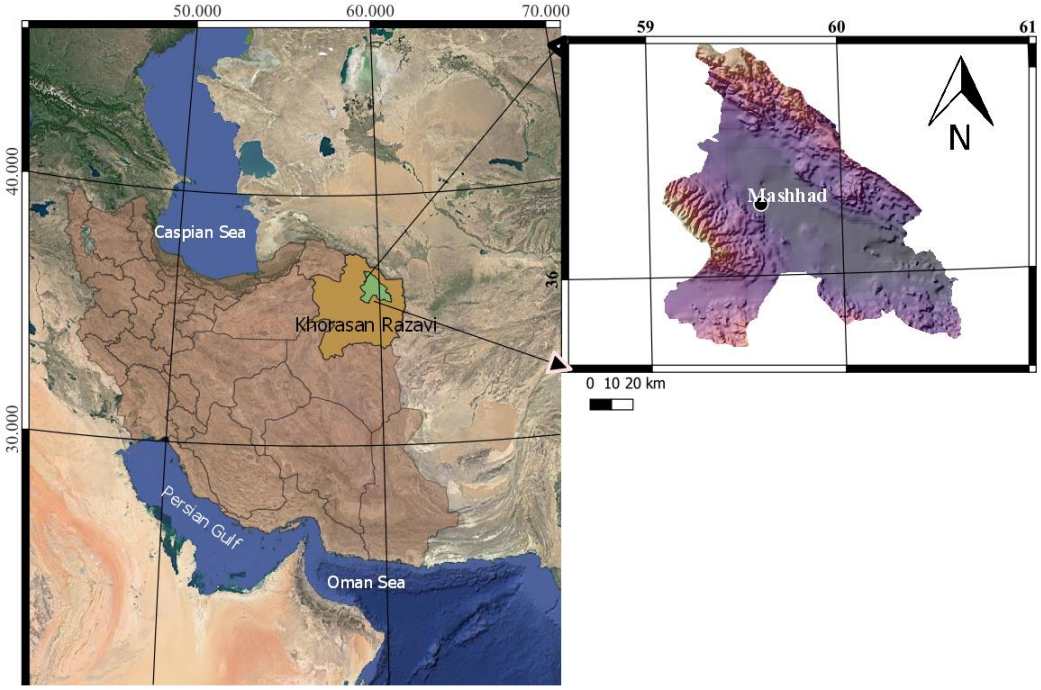


**Fig. 1.** Location of Mashhad Area in Iran and Khorasan Razavi province, as well as the elevation

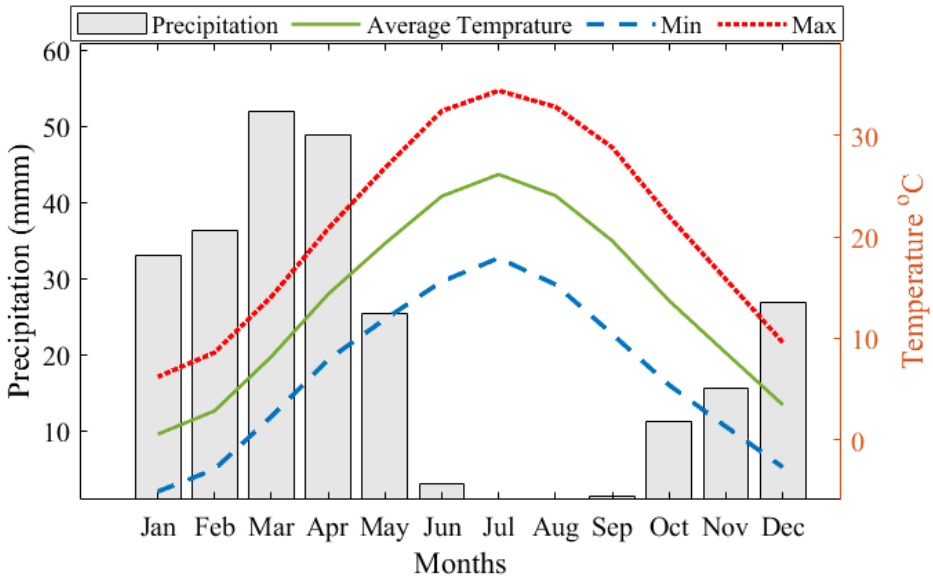


**Fig. 2.** Trend of temperature and precipitation in Mashhad Area

## Data Collection

In this study, we considered using six potential indicators, including enhanced vegetation index (EVI), Vegetation Condition Index (VCI), salinity index (SI), Synthetized Drought Index (SDI), Temperature Condition Index (TCI), and precipitation for May when vegetation growth reaches its maximum size. We used the MODIS satellite EVI product (MOD13Q1), MODIS NDVI product (MOD13A3v006), MODIS Land Surface Temperature (LST) product (MOD11A2), and MODIS MOD13Q1 product for calculating the salinity index from https://MODIS.gsfc.nasa.gov. Precipitation data were obtained for the 83 climate stations in Khorasan Razavi province. The Shuttle Radar Topography Mission (SRTM) 1 Arc-Second was obtained from https://srtm.csi.cgiar.org/. All processes were performed in ENVI 5.3 and ArcGIS 10.3.

## Indicators Utilized

### a) Enhanced Vegetation Index (EVI)

The EVI index is more preferable to the conventional Normalized Vegetation Index (NDVI) since it is not sensitive to vegetation changes, atmospheric conditions and noise. This index is calculated as:

$$EVI = G\frac{NIR-Red}{NIR+C_1Red-C_2Blue+L}$$ (Equation 1)

Where:

NIR, Red, and Blue are fully or partially atmospheric-corrected surface reflectance,

L is the canopy background adjustment for correction of the nonlinear, differential NIR and red radiant transfer through a canopy and

$C_1$ and $C_2$ are the coefficients of the aerosol resistance terms, and

G is the gain or scaling factor.

The coefficients adopted in calculating EVI product are L=1, $C_1$=6, $C_2$=7.5, and G=2.5. (Didan *et al.*, 2015). This index ranges between 0 and 1, with denser vegetation cover obtaining higher values. The MODIS product for 2020 was obtained, which are available for every 16 days, and we used the weighted average method to convert the data into monthly equivalent.

### Vegetation Condition Index (VCI)

The main idea behind this index is the evaluation of vegetation growth in response to climate changes and its evolution in response to the maximum and minimum growth potential defined by ecological constraints (Kogan, 1995). This index is calculated as follows:

$$VCI_i = \frac{NDVI_i-NDVI_{min}}{NDVI_{max}-NDVI_{min}}$$ (Equation 2)

Where:

$VCI_i$ is vegetation condition in the ith year of the study period,

$NDVI_i$ is the NDVI value for each pixel in the ith year,

$NDVI_{max}$ and $NDVI_{min}$ are the maximum and minimum NDVI values in the study period, respectively.

The monthly VCI product was used for the calculation of this index.

### b) Precipitation

A correlation between altitude and precipitation was established between 83 weather stations inside and around the area (Khorasan Razavi province), in order to prepare the interpolated map of precipitation. Fig. 3 shows the correlation between altitude of the weather stations and their corresponding precipitation. The $R^2$ value of 0.71 shows the acceptable level of accuracy.

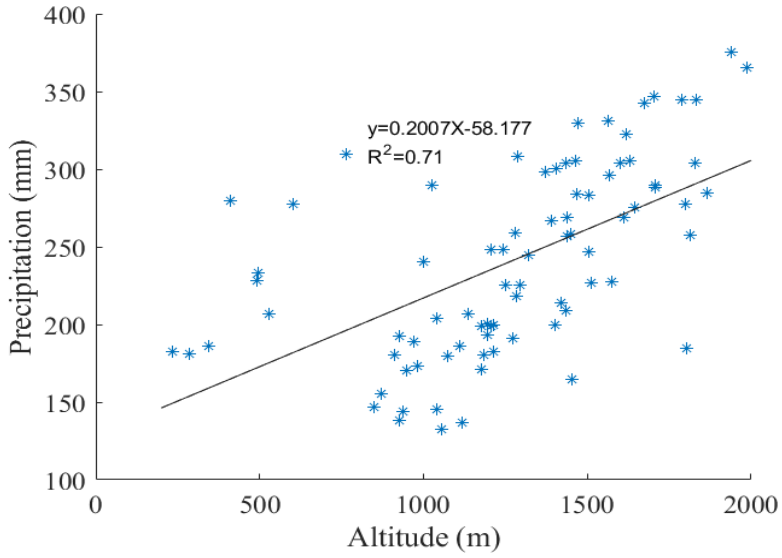


**Fig. 3.** Correlation between altitude and precipitation between 83 stations of the Khorasan Razavi province

### c) Temperature Condition Index (TCI)

The Temperature Condition Index (TCI) (Kogan, 1995) is complementary to the VCI Index to evaluate drought severity. Here, areas with a higher risk of desertification lose soil moisture and display thermal tension at the ground level, which increases air temperature. The MODIS land surface product at the resolution of 1 Km at eight-day intervals was used to calculate this index. The data were converted to the monthly equivalent. TCI is calculated as:

$TCI_i = \frac{LST_{max} - LST_i}{LST_{max} - LST_{min}}$ (Equation 3)

Where:

$TCI_i$ is the temperature condition values in the $i^{th}$ year,

$LST_{max}$ is the maximum ground surface temperature value for each pixel in the study period

$LST_i$ is the ground surface temperature value for each pixel in the ith year, and

$LST_{min}$ is the minimum ground surface temperature value for each pixel in the study period.

Unlike NDVI, in TCI index, the maximum surface temperature values occur in dry years, and the minimum surface temperature values happen in normal years. This index ranges from zero to one, when drought conditions receive the values close to zero and wet years receive the values close to one.

### d) Synthetized Drought Index (SDI)

The synthetized drought index (SDI) was obtained using the principal component analysis (PCA) test in order to remove the iterative information among all other indices. The PCA test was applied on the NDVI and VCI indices as the vegetation assessment component, LST data as the land surface temperature analysis component (TCI index), and precipitation data as the precipitation assessment component and we found the results to be significant for VCI, TCI, and P (similar to the work of Du *et al.* (2013)). Since VCI, TCI and P accounted for the highest total variances (98.8%), they were selected as the candidates for generating SDI map (eq. 4), as:

$SDI = \alpha.VCI + \beta.TCI + \Theta.P$ (Equation 4)

Where: α, β and Θ are the total variance explained by VCI, TCI and P in PCA, respectively.

### e) Salinity Index (SI)

Salinization is a major cause of desertification. Soil salinity increase is attributable to the parent materials, chemicals, improper irrigation and water quality, saline groundwater rise, etc. (Daliakopoulos *et al.*, 2016; Wang *et al.*, 2009). We used the MODIS visible bands which come at 16-day intervals to calculate the salinity index (SI). The data were converted to the monthly equivalent using the weighted average method. Bands 4 (red band) and 6 (blue band) of this product with 500-meter resolution were used. SI is calculated as (Mehta *et al.*, 2013):

$SI = \sqrt{BLUE * RED}$ (Equation 5)

Where: RED and BLUE are the red and blue bands of MODIS images.

### Normalization

In order to combine the RS thematic layers, they must have a common scale of measurement. The process of converting data into a comparable range of values is called standardization. There are several standardization procedures such as Min-Max, Z-score, Median Normalization, Fuzzy Transform, etc. (Jain *et al.*, 2005). We used the Fuzzy transform method for data normalization into a range of 0 and 1. The Fuzzy Transform was first introduced by Zadeh (1996) to convert verbal expressions into mathematical equations. The fuzzy set X has its fuzzy subset *A* which is defined by a membership function $f_A(X)$ which maps each element in *A* onto a real number between 0-1. Since we were only interested in the lower and upper part of the data indicating severe condition conducing for desertification, the Large

and Small fuzzy membership functions in ArcGIS were applied. The Large fuzzy membership function is defined as:

$$f(x) = \frac{1}{1+(\frac{x}{f^2})^{-f^1}}$$ (Equation 6)

Where

$f^1$ is the spread parameter defining the shape and character of the transition zone and

$f^2$ is the midpoint, after which numbers have a higher possibility of becoming a member of the set (Jafari Shalamzari *et al.*, 2019).

And the Small fuzzy membership function is defined as:

$$f(x) = \frac{1}{1+(\frac{x}{f^2})^{f^1}}$$ (Equation 7)

In the smaller function, numbers after the midpoint have a lower possibility of becoming a member of the set. Here, TCI, SDI, VCI and salinity layers were standardized using the large function while EVI and Precipitation layers were standardized using the small function.

## Scaling

The combination of the standardized layers requires identifying the importance of each indicator in the final decision. The Analytic Hierarchical Process (AHP) and the Analytic Network Process (ANP) developed by Saaty (Saaty, 2008) are the widely-used methods. Since the results of the ANP method is more complicated to interpret as compared with the AHP (Görener, 2012), we decided to determine the weight of different indicators using the AHP method. Each indicator was assigned a score between 1 to 9 according to Table 1 by five experts familiar with the topic and the study area. The results were analyzed in Expert Choice 11.0 software. The comparisons are considered to be valis as long as the inconsistency between judgments remain low. This was evaluated using the Consistency Ratio (CR) and since the CR value was less than 10%, all judgements were considered to be valid.

**Table 1.** The scoring scheme used for generating pairwise comparison matrices in the AHP approach (Jafari Shalamzari *et al.*, 2019)

| Scores | Importance |
|---|---|
| 1 | Equally important |
| 3 | Moderately more important |
| 5 | Strongly More Important |
| 7 | Very strongly more important |
| 9 | Extremely more important |
| 2,4,6,8 | Intermediate values between two levels of importance |

## Combination

The final desertification intensity was calculated using the weighed overlay combination as (eq. 8):

$DI = \sum_{i=1}^{n} W_i \times y_i$ (Equation 8)

Where:
$W_i$ is the weight assigned to each layer, and
$y_i$ is the fuzzy layer.
The final map was classified as: 0-0.25 low, 0.25-0.5 moderate, 0.5-0.75 high, 0.75-1 very high.

## Results

### a) Scaling

The results of the AHP method are brought in Table 2 According to the results, precipitation and enhanced vegetation indices (EVI) obtained the highest importance. At the same time, land temperature and VCI are considered to be the least important factors since the area is already experiencing high temperatures. Salinity seems to be of great importance in the region since it received one fourth of the total importance. Given the consistency ratio of 0.06, all comparisons are believed to be valid.

**Table 2.** The resulting weights obtained from the AHP method for the thematic layers for determining desertification intensity in the Mashhad Area of Iran

| Indices | Weights |
|---|---|
| Temperature Condition Index (TCI) | 0.0977 |
| Vegetation Condition Index (VCI) | 0.2582 |
| Enhanced Vegetation Index (EVI), | 0.1846 |
| Synthetized Desertification Index (SDI) | 0.1346 |
| Precipitation | 0.2559 |
| Salinity Index | 0.0644 |
| Total | 1 |
| Consistency Ratio | 0.06 |

Note Enhanced vegetation index (EVI), Vegetation Condition Index (VCI), Synthetized Desertification Index (SDI), Temperature Condition Index (TCI), Precipitation (P), Salinity Index (SI)

## b) Areal Distribution of Thematic Layers

The standardized thematic layers are provided in Fig. 4 and the distribution of the indices are provided in Table 3. As for the TCI, VCI, and SDI, the greatest proportion of the area fell under the no drought to mild drought category indicating lower risk of desertification. However, the synthetized desertification index (SDI) is mainly distributed around the moderate and mild class (~39%). The results of the EVI index also indicated that most of the area has a suitable vegetation density and low risk of desertification. According to Fig. 4, in the SI index, ~98% happened under the low salinity risk.

**Table 3.** Distribution of land area in different classes of desertification assessment indicators in 2020 in Jogatai Area (source Du *et al.* (2013) and Kacem *et al.* (2021)

| *Kacem et al. (2021)* | | | | | *Kacem et al. (2021)* | | | | | |
|---|---|---|---|---|---|---|---|---|---|---|
| Class | Range | TCI | SDI | VCI | Class | Range | EVI | Class | Range | SDI |
| Extreme D. | 0-0.1 | 14.8 | 2.0 | 3.4 | | | | | | |
| | | | | | Very Low D. | 0-0.2 | 0.8 | Low D. | 0-0.17 | 10213.2 |
| Severe D. | 0.1-0.2 | 271.3 | 253.8 | 7.6 | | | | | | |
| | | | | | Low D. | 0.2-0.4 | 69.9 | Moderate D. | 0.17-0.2 | 86.0 |
| Moderate D. | 0.2-0.3 | 1279.2 | 1361.2 | 38.2 | | | | | | |
| | | | | | Moderate D, | 0.4-0.6 | 438.5 | High D. | 0.2< | 37.8 |
| Mild D. | 0.3-0.4 | 3294.7 | 2706.4 | 169.7 | High D. | 0.6-1 | 9817.7 | | | |
| Abnormal D. | 0.4-0.5 | 4532.7 | 2398.6 | 1049.9 | | | | | | |
| No D. | 0.5-1 | 944.6 | 3617.8 | 9058.2 | | | | | | |

Drought (D), Enhanced vegetation index (EVI), Vegetation Condition Index (VCI), Synthetized Drought Index (SDI), Temperature Condition Index (TCI)

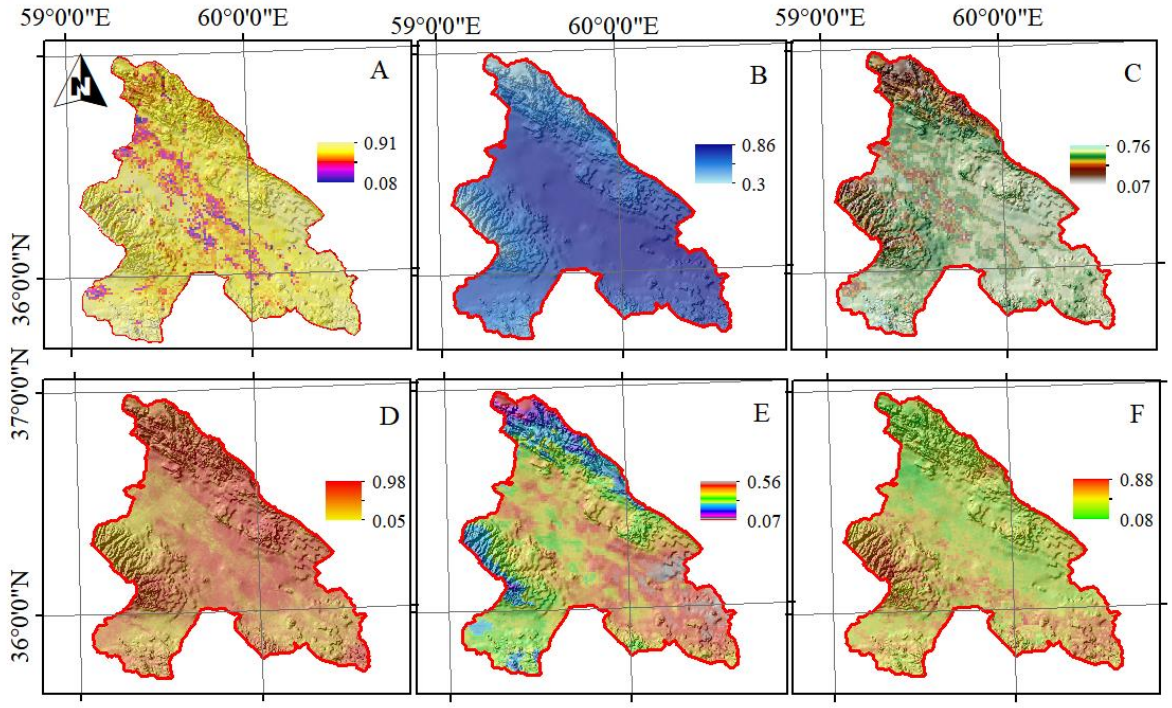


**Fig. 4.** Standardized layers of the thematic maps for evaluating desertification risk in Mashhad county, a) Enhanced vegetation index (EVI), b) Precipitation, c) Vegetation Condition Index (VCI), d) Salinity, e) Temperature Condition Index (TCI) and f) Synthetized Drought Index (SDI)

## c) Fuzzy Overlay

The final results of the Fuzzy overlay are provided in Fig. 5 and Table 4. The final score ranges between 0.29 and 0.63. We divided the whole range of 0-1 into four classes of No risk to High Risk of desertification. The results showed that the greatest parts of the area belong to the moderate risk (~68%) and high risk (30.1) classes of desertification. The highest values were obtained in the eastern and southeastern parts of the area with the lowest level of vegetation density, and high temperature indices. Naturally, the elevations received the lowest values showing an increasing gradient towards the middle plain. Mashhad as the major population center of the area (Fig. 1) is located in the low-risk category; therefore, desertification doesn't seem to be threatening the city at the moment.

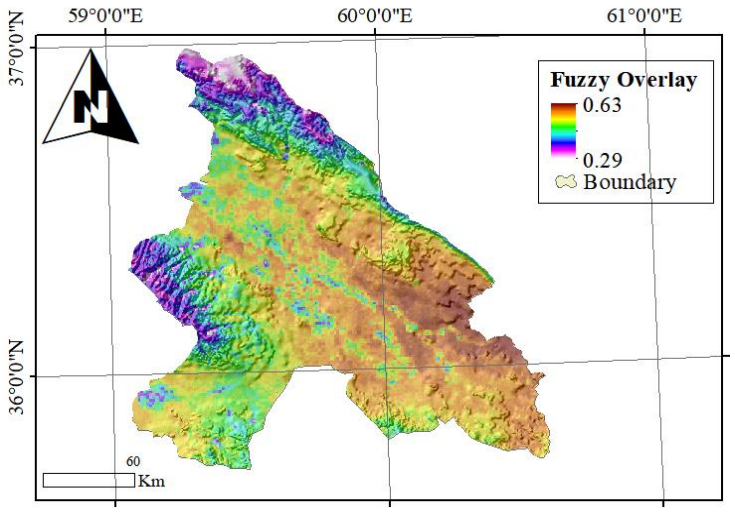


**Fig. 5.** Distribution of desertification sensitivity across the Mashhad county. The layer is superimposed on the hill shade obtained from the STRM 90m DEM.

**Table 4.** Distribution of area among different desertification classes in Mashhad Region

| Class | No. of Pixels | Area ($km^2$) | Relative Percentage |
|---|---|---|---|
| No Sensitivity | 1 | 0.1 | 0.0 |
| Low Sensitivity | 3946 | 208.7 | 2.0 |
| Moderate Sensitivity | 132456 | 7006.9 | 67.9 |
| High Sensitivity | 58705 | 3105.5 | 30.1 |
| Total | 195108 | 10321.2 | 100.0 |

## Discussion

In this research, we used a combination of satellite remote sensing products to evaluate desertification in Mashhad, Khorasan Razavi province, Iran. Based on the expert comparisons and the AHP results, VCI, precipitation and EVI were the most important factors determining desertification intensity in the area. Abdollahi *et al.* (2019a) similarly assigned lower importance values to temperature indices such as LST in Mashhad area.

In terms of the drought indices, we used TCI, VCI and SDI indices. The TCI index which is calculated from the land surface temperature indicates the level of soil moisture concentration. Since higher temperatures result in high evaporation rates, the areas with higher TCI values face severe moisture tension for plant growth and development. Accordingly, most of the area falls into the low-tension classes (no drought to mild drought) and therefore, this index doesn't seem to impose a great limitation. Conversely, Abdollahi *et al.* (2019a) found high TCI values in Mashhad and high soil moisture tension, as conducing factors of desertification.

The vegetation condition index (VCI) compares the current NDVI values to corresponding values in the same time in previous years; therefore, each value is a percentage of the difference between maximum and minimum values in previous years. Again, we obtained high values for this index which indicates the condition is not in favor of desertification. The combination of drought indices in terms of the SDI index (VCI, TCI and precipitation) also didn't indicate a severe drought condition in the year 2020. The Enhanced vegetation index (EVI) which is in fact a complement to the NDVI index, in which it can capture leaf area values and remove background noise, showing that most of the area enjoyed dense to moderately-dense vegetation in 2020. Therefore, vegetation status is also not a source of concern for desertification. The same result was also obtained for salinity in that the largest part of the area happened under the low salinity category. However, Abdollahi *et al.* (2019b) found great variations in EVI index in Mashhad and classified the region as vulnerable to desertification. Their results included the variation of this index over time, but since we only evaluated desertification vulnerability in the year 2020, we did not notice any considerable limitations in terms of vegetation cover.

The final fuzzy overlay map indicated that most of the area is at moderate or high risk of desertification. Those areas having high desertification vulnerability also happened to have higher TCI and SDI values which in combination indicate the harsh condition of the area for vegetation establishment (Yari *et al.*, 2018). The same results were obtained by Sepehr and Parvian (2012) and Sepehr *et al.* (2014). By applying the same methodology, Shiravi and Sepehr (2017) found high vulnerability to desertification in Khorasan Razavi province. Similar to our results, Pashaei *et al.* (2017) by applying the EVI, salinity, and LST index during 2000 to 2013 found that more than 60% of the area is vulnerable to desertification.

Our results indicated a great danger of being exposed to desertification in Mashhad. Desertification is in fact anthropogenic with the expansion of residential areas, rain-fed farming, over-grazing and activities related to water resources such as over-exploitation of

water resources and improper irrigation activities especially in eastern areas with higher salinity levels as the main factors. According to Nikou (2017), land-use change (reduction of arable lands in favor of residential areas) is a major factor helping desertification in this area. Likewise, Tervonen *et al.* (2015) believe that Khorasan Razavi is ecologically vulnerable to desertification. Jafari *et al.* (2019), Davari *et al.* (2017) and Feyzi Koushki *et al.* (2019) introduced human activities, climate change, water, socio-economic criteria, agricultural activities, vegetation, soil and geology, and erosion as the main causes of desertification in Khorasan Razavi province, Iran.

## Conclusion

In this research, we used a combination of satellite remote sensing products to evaluate desertification in Mashhad county of Khorasan Razavi province. Our results indicated a great danger of being exposed to desertification in Mashhad. However, the main limitation behind using the remote-sensing products in evaluating desertification is the coarse resolution of most of the indices which could result in the mismatch between different layers and hence over or underestimation of the risk. In order to obviate the issue, during the field survey, desertification was evaluated in more than 200 points and based on the expert opinion, a score between 0 and 1 was assigned to each location. The comparison between the results and the ground truth data indicated high compatibility (kappa value of >0.70). Therefore, it seems our results are technically sound and reliable. In conclusion, we can see the area is vulnerable to desertification and the land managers need to devise suitable plans not only to tackle the issue, but also to mitigate possible outcomes in the long run.

## Acknowledgement

I would like to thank Hakim Sabzevari University, Iran for its support for making this research possible.

## References

Abdollahi, A., Nezhad, M. P., Pradhan, B., 2019a. Determining the desertification risks of the Mashhad regions using integrated indices based on the AHP method. 2019 13th International Conference on Sensing Technology (ICST), 2-4 Dec. 2019. 1-6.

Abdollahi, A., Nezhad, M. P., Pradhan, B., 2019b. Investigation of the Vegetation Cover and the Vulnerability of the Mashhad Regions to Desertification by Using MODIS Image and EVI. 2019 IEEE International Conference on Cybernetics and Computational Intelligence (CyberneticsCom), 22-24 Aug. 2019. 46-49.

Aixia, L., Changyao, W., Jing, W., Xiaomei, S., 2007. Method for remote sensing, monitoring of desertification based on MODIS and NOAA/AVHRR data. Trans. Chin. Soc. Agric. Eng, 23 145-150.

Akbari, M., Memarian, H., Neamatollahi, E., Jafari Shalamzari, M., Alizadeh Noughani, M., Zakeri, D., 2021. Prioritizing policies and strategies for desertification risk management using MCDM–DPSIR approach in northeastern Iran. Environ. Dev. Sustain., 23 (2), 2503-2523.

Akbari, M., Shalamzari, M. J., Memarian, H., Gholami, A., 2020. Monitoring desertification processes using ecological indicators and providing management programs in arid regions of Iran. Ecol. Indic., 111 106011.

Alamdarloo, E. H., Manesh, M. B., Khosravi, H., 2018. Probability assessment of vegetation vulnerability to drought based on remote sensing data. Environmental monitoring and assessment, 190 (12), 1-11.

Albalawi, E. K., Kumar, L., 2013. Using remote sensing technology to detect, model and map desertification: A review. J. Food Agric. Environ., 11 (2), 791-797.

Bezerra, F. G. S., Aguiar, A. P. D., Alvalá, R. C. S., Giarolla, A., Bezerra, K. R. A., Lima, P. V. P. S., do Nascimento, F. R., Arai, E., 2020. Analysis of areas undergoing desertification, using EVI2 multi-temporal data based on MODIS imagery as an indicator. Ecol. Indic., 117 106579.

Daliakopoulos, I., Tsanis, I., Koutroulis, A., Kourgialas, N., Varouchakis, A., Karatzas, G., Ritsema, C., 2016. The threat of soil salinity: A European scale review. Sci. Total Environ., 573 727-739.

Davari, S., Rashki, A., Akbari, M., Talebanfard, A., 2017. Assessing intensity and risk of desertification and management programs (Case

study: Ghasemabad plain of Bajestan, Khorasan Razavi Province). Desert Manage., 5 (9), 91-106.

Didan, K., Munoz, A. B., Solano, R., Huete, A. 2015. MODIS vegetation index user's guide (MOD13 series). University of Arizona: Vegetation Index and Phenology Lab.

Du, L., Tian, Q., Yu, T., Meng, Q., Jancso, T., Udvardy, P., Huang, Y., 2013. A comprehensive drought monitoring method integrating MODIS and TRMM data. Int J Appl Earth Obs Geoinf, 23 245-253.

Egidi, G., Salvati, L., 2020. Desertification risk, economic resilience and social issues: From theory to practice. Chinese Journal of Population, Resources and Environment, 18 (2), 155-163.

Elhadi, E. M. A., Dano, U. L., 2020. Desertification Assessment and Mapping in Northern Shaanxi Province: A GIS-based and Remote Sensing Approach. Disaster Adv., 13 (2), 1-10.

Fathi, A., Jafari, R., Soltani, S., 2015. Performance comparison of MEDALUD, MICD and FAO-UNEP desertification mapping models in the desertification hotspot of Jarghoyeh region, Isfahan province. J. Agr. Sci. Tech-Iran, 19 (71), 299-310.

Fathizad, H., Ardakani, M. A. H., Mehrjardi, R. T., Sodaiezadeh, H., 2018. Evaluating desertification using remote sensing technique and object-oriented classification algorithm in the Iranian central desert. J. Afr. Earth Sci. 145 115-130.

Feyzi Koushki, F., Akbari, M., Memarian, H., Azamirad, M., 2019. Identifying and ranking important factors of desertification in Khorasan Razavi Province using Delphi method. J. Geogr. Environ. Hazards, 8 (3), 225-205.

Gad, A., Lotfy, I., 2008. Use of remote sensing and GIS in mapping the environmental sensitivity areas for desertification of Egyptian territory. Solid Earth Discuss, 3(2), 41-85.

Görener, A., 2012. Comparing AHP and ANP: an application of strategic decisions making in a manufacturing company. Int. J. Bus. Soc. Sci. Res., 3 (11), 194-208.

Jafari, H., Akbari, M., Kashki, M., Badiee Nameghi, S., 2019. An efficiency comparison of the IMDPA and ESAs models on desertification risk management in arid regions of southern Khorasan Razavi, Iran. Arid Biome Sci. Resour. J., 9 (1), 39-54.

Jafari, M., Gholami, A., Khalighi Sigaroudi, S., Alizadeh Shabani, A., Arzani, H., 2018. Site selection for rainwater harvesting for wildlife using multi-criteria evaluation (MCE) technique and gis in the kavir national park, Iran. J. Rangel. Sci., 8 (1), 77-92.

Jafari Shalamzari, M., Zhang, W., Gholami, A., Zhang, Z., 2019. Runoff Harvesting Site Suitability Analysis for Wildlife in Sub-Desert Regions. Water, 11 (9), 1944.

Jain, A., Nandakumar, K., Ross, A., 2005. Score normalization in multimodal biometric systems. Pattern Recogn., 38 (12), 2270-2285.

Kacem, H. A., Fal, S., Karim, M., Alaoui, H. M., Rhinane, H., Maanan, M., 2021. Application of fuzzy analytical hierarchy process for assessment of desertification sensitive areas in North West of Morocco. Geocarto Int., 36 (5), 563-580.

Kjellen, B., 2003. The saga of the Convention to Combat Desertification: the Rio/Johannesburg process and the global responsibility for the drylands. Rev. Eur. Comp. & Int'l Envtl. L., 12 127.

Kogan, F. N., 1995. Application of vegetation index and brightness temperature for drought detection. Adv. Space Res., 15 (11), 91-100.

Kosmas, C., Kirkby, M. J., Geeson, N. (eds.) 1999. Medalus Project: Mediterranean Desertification and Land Use. Manual on key indicators of Desertification and Mapping Environmentally Sensitive Areas., Brussels, Belgium: Publication of European Union.

Kumar, B. P., Babu, K. R., Rajasekhar, M., Ramachandra, M., 2019. Assessment of land degradation and desertification due to migration of sand and sand dunes in Beluguppa Mandal of Anantapur district (AP, India), using remote sensing and GIS techniques. J. Indian Geophys. Union, 23 (2), 173-180.

Lin, M. L., Chen, C. W., Wang, Q. B., Cao, Y., Shih, J. Y., Lee, Y. T., Chen, C. Y., Wang, S., 2009. Fuzzy model-based assessment and monitoring of desertification using MODIS satellite imagery. Eng. Comput., 26 (7), 745-760.

Liu, Y., Dang, C., Yue, H., Lyu, C., Dang, X., 2021. Enhanced drought detection and monitoring using sun-induced chlorophyll fluorescence over Hulun Buir Grassland, China. Sci. Total Environ., 770 145271.

Ma, H., Zhao, H., 1994. United Nations: Convention to combat desertification in those countries experiencing serious drought and/or desertification, particularly in Africa. Int. Legal Mater, 33 1328-1382.

Mehta, M., Saha, S., Agrawal, S., 2013. Evaluation of Indices and Parameters Obtained from Optical and Thermal Bands of Landsat 7 ETM+ for Mapping of Salt-Affected Soils and Water-Logged Areas. Asian J. Geoninf., 12 (4).

Mouat, D. A., Hutchinson, C. F. 2012. Desertification in Developed Countries: International Symposium and Workshop on Desertification in Developed Countries: Why Can't We Control It?, Springer Science & Business Media.

Murray, N. J., Keith, D. A., Bland, L. M., Ferrari, R., Lyons, M. B., Lucas, R., Pettorelli, N., Nicholson, E., 2018. The role of satellite remote sensing in structured ecosystem risk assessments. Sci. Total Environ., 619 249-257.

Nikou, S., 2017. Impacts of land use changes on Technogenic desertification in Mashhad city. Desert Ecosys. Eng. J., 5 (13), 81-90.

Oldeman, L., Hakkeling, R., Sombroek, W., Batjes, N. 1991. Global assessment of human-induced soil degradation (GLASOD). World map of the status of human-induced soil degradation. Wageningen, Netherlands: Winand Staring Centre–ISSSFAO–ITC.

Pashaei, M., Rashki, A., Sepehr, A., 2017. An integrated desertification vulnerability index for Khorasan-Razavi, Iran. Nat. Resour. Conserv., 5 (3), 44-55.

Saaty, T. L., 2008. Decision making with the analytic hierarchy process. Int. J. Serv. Sci., 1 (1), 83-98.

Sepehr, A., Parvian, N., 2012. Desertification vulnerability mapping and prioritize confronting strategies in Khorasan Razavi province based on the Nartbh Pramsh algorithm. Earth Sci. Res. J., 8 58-71.

Sepehr, A., Zucca, C., Nowjavan, M. R., 2014. Desertification Inherent Status Using Factors Representing Ecological Resilience. Brit. J. Env. Clim. Change, 4 (3), 279.

Shihab, T. H., Al-hameedawi, A. N., 2020. Desertification Hazard Zonation in Central Iraq Using Multi-criteria Evaluation and GIS. J. Indian Soc. Remote. Sens., 48 (3), 397-409.

Shiravi, M., Sepehr, A., 2017. Fuzzy Based Detection of Desertification-Prone Areas: A Case Study in Khorasan-Razavi Province, Iran. Nat. Res. Conserv.

Sivakumar, M., 2007. Interactions between climate and desertification. Agric. For. Meteorol., 142 (2-4), 143-155.

Sörensson, A. A., Ruscica, R. C., 2018. Intercomparison and uncertainty assessment of nine evapotranspiration estimates over South America. Water Resour. Res., 54 (4), 2891-2908.

Tervonen, T., Sepehr, A., Kadziński, M., 2015. A multi-criteria inference approach for anti-desertification management. J. Environ. Manage., 162 9-19.

Vogt, J., Safriel, U., Von Maltitz, G., Sokona, Y., Zougmore, R., Bastin, G., Hill, J., 2011. Monitoring and assessment of land degradation and desertification: towards new conceptual and integrated approaches. Land Degrad. Dev, 22 (2), 150-165.

Wang, L., Seki, K., Miyazaki, T., Ishihama, Y., 2009. The causes of soil alkalinization in the Songnen Plain of Northeast China. Paddy Water Environ., 7 (3), 259-270.

Yari, R., Gholami, A., Jafari Shalamzari, M., Heshmati, G. A., 2018. Evaluation of Distance and Quadratic Indices for Determination of Plant Species Distribution Pattern in Khoosef Rangelands, Birjand, Iran. J. Rangel. Sci., 8 (4), 373-382.

Zadeh, L. A., 1996. Fuzzy sets. Fuzzy sets, fuzzy logic, and fuzzy systems: selected papers by Lotfi A Zadeh. World Scientific.

# ارزیابی حساسیت شهرستان مشهد به بیابان‌زایی با استفاده از روش ترکیب فازی

**مصطفی دستورانی**

استادیار، دانشکده جغرافیا و علوم محیط زیست، دانشگاه حکیم سبزواری، سبزوار، ایران، پست الکترونیک: m.dastorani@hsu.ac.ir

**چکیده.** در این پژوهش، از شش شاخص سنجش از دور MODIS برای ارزیابی آسیب‌پذیری شهرستان مشهد در ایران به بیابان‌زایی استفاده شده است. شاخص‌های ارتقا یافته پوشش گیاهی (EVI)، شاخص شرایط پوشش گیاهی (VCI)، شاخص شوری (SI)، شاخص ترکیبی خشکسالی (SDI)، شاخص شرایط دمایی (TCI) و شاخص بارش ماه اردیبهشت سال ۱۴۰۰ که پوشش گیاهی در اوج رویش خود است در نظر گرفته شدند. لایه‌های اطلاعاتی با استفاده از روش تبدیل فازی استانداردسازی شده و با استفاده از روش سلسله مراتبی AHP وزن‌دهی شدند. از نظر شاخص‌های TCI، VCI و SDI بیشترین بخش منطقه در کلاس بدون خشکسالی تا خشکسالی خفیف قرار گرفتند که نشان دهنده خطر کم بیابان زایی می‌باشد. اما، شاخص ترکیبی خشکسالی (SDI) عمدتا در کلاس های متوسط تا شدید (۳۹٪) قرار گرفت. نتایج شاخص EVI نیز نشان داد که بیشتر منطقه تراکم خوبی از نظر پوشش گیاهی و خطر بیابان زایی پایینی داشته است. از نظر شاخص شوری، نزدیک به ۹۸ درصد در کلاس بدون شوری قرار گرفت. بر اساس نتایج بدست آمده از روش AHP بارش (۰/۲۵)، VCI (۰/۲۵)، EVI (۰/۱۸)، و SDI (۰/۱۳) بیشترین اوزان را داشته‌اند. مقدار نهایی شاخص آسیب پذیری بین ۰/۲۹ تا ۰/۶۳ قرار گرفت. نتایج نشان می‌دهد که بیشترین قسمت منطقه در کلاس حساسیت متوسط (۶۸ درصد) و زیاد (۳۰/۱ درصد) بوده است. بیشترین مقدار در بخش‌های شرقی و جنوب شرقی منطقه رخ داده که کمترین تراکم پوشش گیاهی و بیشترین مقادیر شاخص دمایی را داشته‌اند. طبیعتا، ارتفاعات کمترین میزان (۰/۲۹) را به خود اختصاص داده‌اند که به سمت دشت میانی مقادیر رو به افزایش بوده است. مقایسه بین نتایج بدست آمده و حقایق زمینی نشان از شاخص کاپای بیش از ۰/۷۰ و سازگاری بالای نتایج بوده است. شهر مشهد به عنوان یک مرکز جمعیتی مهم در کلاس پایین حساسیت قرار داشته و بیابان‌زایی در حال حاضر به نظر تهدیدی برای این شهر نمی‌یابد.

**کلمات کلیدی:** تخریب، کاربری زمین، پوشش گیاهی، شوری، خراسان